Zero and Off-Zero Critical Concentrations in Systems Containing Polydisperse Polymers† with Very High Molar Masses. 2. The System Water−Poly(vinyl methyl ether)

H. Schäfer-Soenen, R. Moerkerke, H. Berghmans,* and R. Koningsveld

Laboratory for Polymer Research, Catholic University Leuven, B-3001 Heverlee, Belgium

K. Dušek and K. Šolc‡

Institute of Macromolecular Chemistry, Academy of Science of the Czech Republic, 162 06 Prague 6, Czech Republic

Received January 25, 1996; Revised Manuscript Received November 13, 1996⊗

ABSTRACT: Cloud-point curves by DSC measurements at different scanning rates on solutions of two samples of poly(vinyl methyl ether) in water show two minima in a temperature−composition plot. The significance of the data was confirmed by static measurements of the coexisting-phase compositions and phase-volume ratios. A thermodynamic analysis in terms of a strongly concentration-dependent interaction parameter leads to the conclusion that the system H_2O/PVME exhibits so-called type III behavior. For polymers of infinite molar mass, such behavior is characterized by the occurrence of two off-zero critical concentrations, in addition to the usual zero critical concentration marking the Θ state.

Introduction

When solutions of polymers with very high molar mass show partial miscibility, the liquid−liquid critical state usually occurs at a very small polymer concentration. The latter tends to zero if the molar mass goes to infinity (Θ state).[1] Indications of possible complications with respect to this generally accepted rule have been reported occasionally,[2−6] and their origin could be related to a strong dependence of the interaction parameter on concentration. This feature has been the subject of a recent phenomenological analysis in which three types of limiting critical behavior could be distinguished.[7] The above mentioned "classic" Θ behavior (type I) is characterized by a limiting critical concentration for infinite molar mass, φ_L, equal to zero. With type II, a single off-zero limiting critical concentration, φ_L , occurs at non-Θ conditions; with type III, there are two off-zero limiting critical concentrations, in addition to the usual zero critical concentration.

Systems in which such phenomena are believed to occur comprise: benzene/polyisobutene,[2,4] aliphatic alcohol/poly(2-hydroxyethyl methacrylate),[3] diphenylether/polyisobutene,[5] water/poly(*N*-isopropylacrylamide),[6] 2-nonanone/poly(methyl methacrylate),[8] and water/poly(vinyl methyl ether).[9] Recent experimental work has provided strong indications for the latter system, H_2O/PVME, to be a case in point for type III behavior. It is the objective of this paper to present additional results.

Types of Limiting Critical Behavior

The liquid−liquid critical state in solutions of a polydisperse polymer in a solvent is determined by the spinodal (1) and critical (2) conditions:[10−13]

$$(m_1\varphi_1)^{-1} + (m_{w2}\varphi_2)^{-1} + (\partial^2\Gamma/\partial\varphi_2^{\,2})_{p,T} = 0 \qquad (1)$$

$$(m_1\varphi_1^{\,2})^{-1} - \xi_2(m_{w2}\varphi_2^{\,2})^{-1} + (\partial^3\Gamma/\partial\varphi_2^{\,3})_{p,T} = 0 \qquad (2)$$

The liquid is considered to be built up of N identical basic volume units (BVU), m_1 of which are occupied by each of the solvent molecules, while an ith species polymer chain needs m_{2i} BVU's. The weight average over all species i is m_{w2}. The concentration variables φ_1 and φ_2 are volume fractions (of solvent and polymer, respectively), but they may also be treated as weight fractions, in which case N stands for the total mass of the system and the BVU is a mass unit. The symbol ξ_2 represents the ratio of z-average to weight-average molar masses of the polymer.

Equations 1 and 2 can be derived from the Flory−Huggins−Staverman[1,14−19] expression for ΔG, the Gibbs free energy of mixing:

$$\Delta G/NRT = (\varphi_1/m_1)\ ln\ \varphi_1 + \sum(\varphi_{2i}/m_{2i})\ ln\ \varphi_{2i} + \Gamma(T,\varphi_2,p) \qquad (3)$$

where φ_{2i} and m_{2i} are the volume fraction and BVU number of species i in the polymer, respectively; $\varphi_2 = \sum\varphi_{2i}$. The function Γ is here used to accommodate all conceivable amendments the first two combinatorial terms might need in actual cases. We assume Γ to be independent of polymer molar mass since the emphasis here is on limiting critical behavior at molar mass tending to infinity.

Equations 1 and 2 can be rearranged into

$$1/m_{w2} = -\varphi_2[(m_1\varphi_1)^{-1} + (\partial^2\Gamma/\partial\varphi_2^{\,2})_{p,T}] \qquad (4)$$

$$\xi_2/m_{w2} = \varphi_2^{\,2}[(m_1\varphi_1^{\,2})^{-1} + (\partial^3\Gamma/\partial\varphi_2^{\,3})_{p,T}] \qquad (5)$$

and it is seen that, for $m_{w2} = \infty$ at finite ξ_2, both expressions indicate $\varphi_2 = 0$ to present the (usual) zero critical concentration under Θ conditions.

† Dedicated to Professor Werner Borchard (Duisburg) on the occasion of his 60th birthday.

‡ On leave of absence from Central Michigan University, Department of Physics, Mt. Pleasant, MI 48859.

⊗ Abstract published in *Advance ACS Abstracts,* January 1, 1997.

S0024-9297(96)00114-3 CCC: $14.00

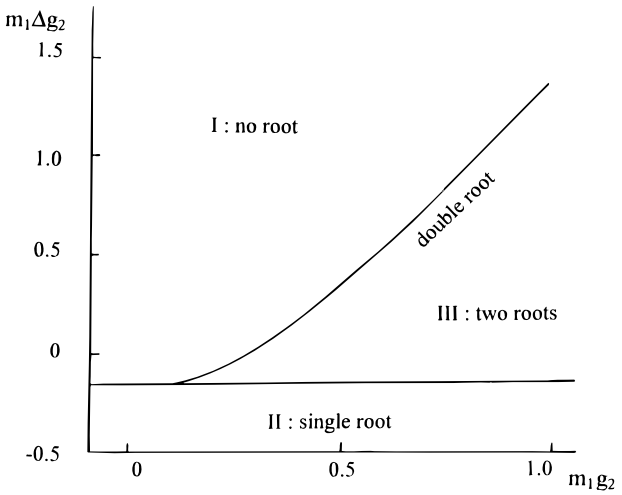

Figure 1. Regions in interaction−coefficient space of types I−III limiting critical behavior. The root classification concerns the off-zero types only.

In the original treatment by Flory and Huggins, Γ is a Van-Laar (VL) type interaction term

$$\Gamma_{VL} = \chi(T)\varphi_1\varphi_2 \tag{6}$$

in which the interaction parameter χ depends solely on temperature.[1] In that case, $\partial^2\Gamma_{VL}/\partial\varphi_2^2 = -2\chi$, and $\partial^3\Gamma_{VL}/\partial\varphi_2^3 = 0$. The classic Θ state is thus the only possibility with (6) since both (4) and (5) must be obeyed at $\chi = 0.5$. The expressions between square brackets in (4) and (5) then have no physically meaningful roots.

Usually, χ is found to depend on φ_2, the dependence of which a number of molecular reasons may be advanced, such as (a) disparity in size and shape among solvent molecules and repeat units in the polymer chains,[20,21] (b) change of free volume with concentration,[22−24] (c) nonuniform segment density at low polymer concentration,[25,26] (d) distribution of free solvent molecules among self-associated complexes and solvated polymer segments.[8,27−29]

All of these factors have been shown to possibly give rise to strong enough $\chi(\varphi_2)$ functions to introduce extra, off-zero roots for the expressions between brackets in (4) and (5). The mathematical form for $\chi(\varphi_2)$ differs from case (1) to (4), but it can usually be developed in a power series in φ_2, the meaning of the coefficients depending on the case considered.

In a recent paper[7] we described a phenomenological analysis of the situation in which the precise molecular meaning of the coefficients is left open:

$$\Gamma(T,\varphi_2) = [g_0(T) + g_1\varphi_2 + g_2\varphi_2^2]\varphi_1\varphi_2 \tag{7}$$

with

$$g_0(T) = g_{0s} + g_{0h}/T \tag{7a}$$

The results of this analysis are summarized in Figure 1 in coordinates of $m_1(g_2-g_1)$ against m_1g_2. There are three areas pertinent to the occurrence of either no root, one root, or two roots of the expressions between square brackets in (4) and (5), to be distinguished as types I, II, and III.

Figure 2, parts I−III, shows representative strictly binary examples for each of the three types in a lower-critical-miscibility situation ($g_{0h} < 0$.[30] With type I a single limiting critical point (at infinite m_2) occurs at

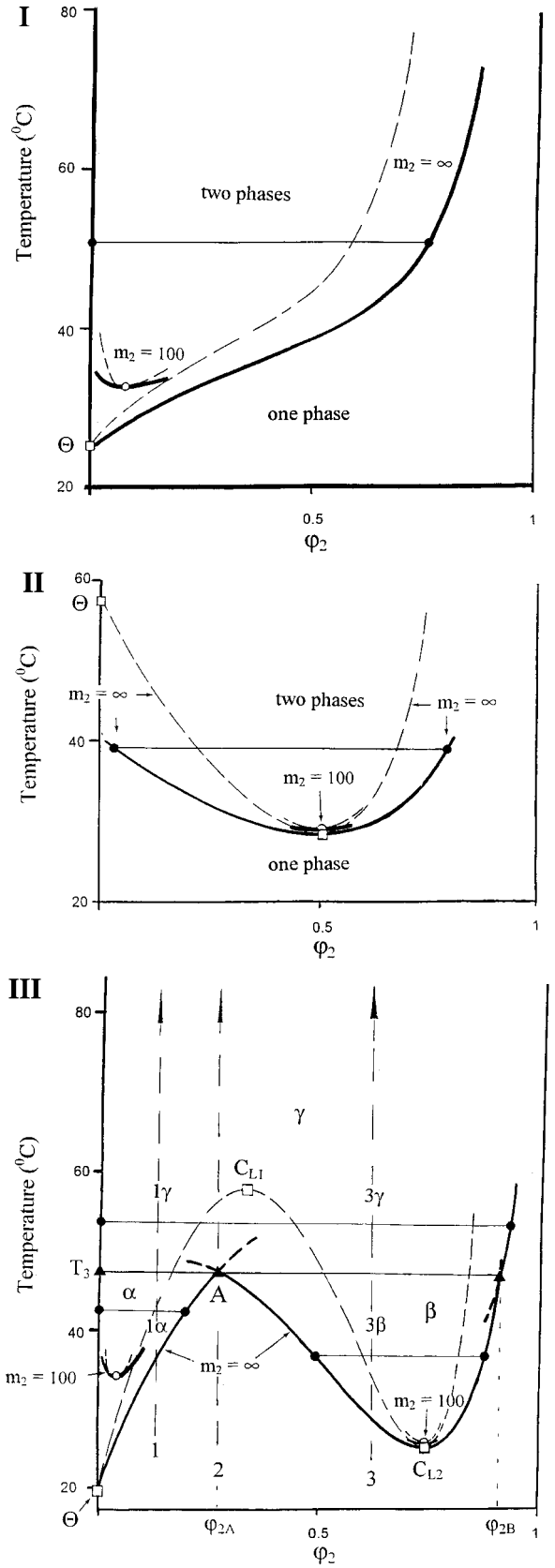

Figure 2. Demixing patterns in strictly binary polymer solutions calculated with eqs 1−3 and 7 for $m_1 = 1$, $m_2 = 100$, and $m_2 = \infty$ (for $m_2 = 100$ only parts of the curves are shown): $g_{0s} = 6.3$, $g_{0h} = -1700$ K. Limiting critical point, □; critical point, ○; tie lines: −●−●−; spinodal, dashed curve; binodal, heavy curve; (I) type I, classic Θ behavior, $g_1 = 0.1$, $g_2 = 0.3$; (II) type II behavior, $g_1 = {}^2/_3$, $g_2 = 0$; (III) type III behavor, $g_1 = -0.0125$, $g_2 = 1.25$. The two two-phase areas α and β are separated from the third one, γ, by the three-phase line at T_3: −▲−▲−▲−.[31]

Table 1. Molecular Characteristics of the PVME Samples

PVME	M_n (kg/mol)	M_w (kg/mol)	M_z (kg/mol)	M_w/M_n	M_z/M_w
1	11	28	80	2.5	2.8
2	19	147	988	7.8	6.7

$\varphi_{2L} = 0$ under Θ conditions, at which the second osmotic virial coefficient, A_2, equals 0.[1] The miscibility gap shifts to higher temperatures with decreasing finite chain length. Type II behavior is characterized by a an off-zero limiting critical point (square symbol), where spinodal and binodal have a common horizontal tangent, and at which $A_2 \neq 0$. The spinodal passes through the Θ point at $\varphi_2 = 0$ and $A_2 = 0$ and coincides with the T axis at $T > \Theta$. The limiting binodal appears to reach the T axis at $\varphi_2 = 0$ at $T < \Theta$, above which temperature its left-hand branch also follows the T axis. In this respect the situation resembles that of type I. Note that (finite) molar mass has little influence on the off-zero critical point (cp) unless m_2 becomes very small.

A type III limiting spinodal has two extrema, one of which (C_{L1}) refers to an unstable limiting cp while the other, stable one (C_{L2}) has features similar to that of type II. As in type I, the Θ state will for finite m_2 transform into a third, stable off-zero cp. The miscibility gap now has three two-phase areas (α, β and γ), one of which (α) shows a chain-length dependence comparable to that of type I. Gap α decreases in size and eventually vanishes into the main one when m_2 is decreased. The chain-length dependence of gap β is similar to that of type II.

It is seen in Figure 1 that the three types may go over into one another. For instance when, upon a change of parameters in $\Gamma(\varphi_2)$, the two off-zero limiting cp's vanish via coalescence in a double cp, type III becomes type I. The single φ_{2L} in type II may either split into two (type III) or shift to lower φ_2 until it equals zero (type I).

In strictly binary systems the two lower two-phase areas (α and β in Figure 2III) are separated from the upper one (γ) by a horizontal line at T_3, which connects the compositions of three phases in nonvariant equilibrium. The three phases cannot be observed simultaneously at T_3, but the existence of the nonvariance is unambiguously revealed by a sudden jump of one of the coexisting-phase concentrations when, upon heating a system within either α or β, T_3 is reached and γ is entered.[31]

The polymer samples used in the experimental illustration of these considerations have wide molar-mass distributions. The three-phase line is then transormed into a three-phase triangle which, however, can be estimated to be so shallow (a few tenths of a degree) that the above-mentioned concentration jump must still be expected to occur. When a system within gap α is allowed to phase separate in such quasi-binary solutions, the overall polymer concentrations of the coexisting phases move closer together when the polymer concentration in the initial system is increased.[32,33]

Experimental Section

The PVME samples and their characterization were received from BASF (Ludwigshafen, Germany). PVME was prepared by cationic polymerization. The weight-average molecular masses for the different samples were determined by light scattering, with toluene as the solvent. Molecular polydispersity was investigated by gel permeation chromatography (GPC), with THF as eluent. Since the GPC calibration was based on polystyrene standards, the average molecular masses, presented in Table 1, have been calculated from the GPC values with a method developed in-house.[9]

The tacticity of the samples was investigated by ^{1}H- and ^{13}C-NMR. Both polymers show similar triad fractions: syndiotactic = 0.11, heterotactic = 0.51, isotactic = 0.38.

To prepare homogeneous solutions of PVME in deionized water, the appropriate amounts of PVME and water were mixed, and these mixtures were left at room temperature for a period of weeks. This procedure results in homogeneous samples that give very reproducible data. Concentrations are indicated as weight fraction of PVME.

Two types of differential scanning calorimeters were used: a Perkin-Elmer DSC7 and a Setaram DSC111-Micro calorimeter. Calibration was performed with indium (T_m =156.6 °C) and sodium sulfate decahydrate (T_m = 32.38 °C).

Measurements with the DSC7 were performed at a scanning rate of 3 °C/min, and experiments with the DSC111 were carried out at a scanning rate of 0.1 °C/min.

Samples of about 30 and 100 mg were used with the DSC7 and DSC111, respectively.

The transparency of the samples was followed during heating at 0.1 °C/min by monitoring the transmitted light intensity. The temperature at the first deviation of the transmitted light intensity from linearity was taken as the cloud point of the corresponding solution (T_c). The procedure allows us to measure mixtures in a broad concentration range.

For solutions with concentrations between 4% and 10%, a separation into two transparent layers could be realized by isothermal annealing at constant temperature. The volume ratio of these two layers was investigated by a technique reported elsewhere.[34]

The coexisting polymer concentrations were determined by refractive index measurements at 25 °C using an Abbé refractometer.[35] A refractive index−concentration plot was constructed that was found to be linear between 0% and 50% of PVME.

Results

1. Calorimetry. The possibility of analyzing liquid−liquid demixing by calorimetric measurements has been discussed in the literature[36] and has been applied to many different polymer−solvent systems.[37−45] These investigations have illustrated the reliability of the experimental method which was therefore applied to the system PVME/water. Two different scanning calorimeters were used, so that experimental data could be collected at very different scanning rates. This provided information on the influence of the scanning rate. The similarity of the data obtained at different scanning rates supports the significance of the observations.

Temperature−Concentration Diagram. The demixing of the system PVME/water is endothermic[35,44] as confirmed by the endothermic signals obtained on heating. Typical examples of DSC curves are presented in Figure 3. In the following we discuss T_d, the temperature at the onset of the endotherm (demixing temperature) and T_p, the peak temperature as a function of the polymer concentration for the two PVME-samples (Figure 4). The demixing curve obtained by plotting T_d *vs* concentration strongly indicates the occurrence of two minima, a phenomenon which is most marked for the higher molecular weight sample, PVME 2.

The peak temperature, T_p, shows little concentration dependence in the investigated concentration range. The scanning rate has an influence on these data: a decrease from 3 to 0.1 °C/min results in a lowering of T_p and T_d. The concentrations of the two minima in the demixing curves are not noticeably altered by a change of heating rate.

Shape of the Endotherms. The shape of the endotherms and their dependence on concentration and

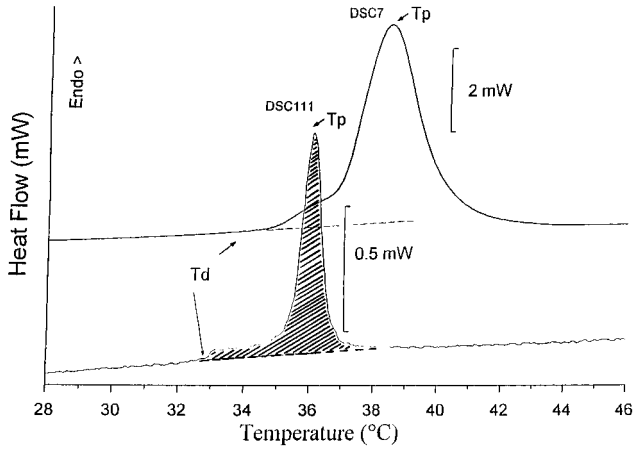

Figure 3. DSC heating scans of a 10 wt % PVME 2 solution in water: scanning rates, 3 °C/min (DSC7), 0.1 °C/min (DSC111); estimated base line, – – –; demixing temperature, T_d, peak temperature, T_p.

molecular mass is in agreement with the occurrence of a bimodal miscibility gap. It has been shown[36] that the width of a DSC signal observed by demixing depends on the shape of the phase boundaries and, hence, on the location of the coexistence curves. This is illustrated in Figure 5, which represents two possible demixing curves, and in Figure 6, which shows the corresponding simulated DSC curves.

If a miscibility gap exhibits two well-separated minima, the DSC traces have a more complex appearance, depending on the concentration. Two endotherms will be observed if the concentration is such that, upon heating, either of the miscibility gaps α or β is entered. A single peak will be found if the concentration equals that of the intersection A of the phase boundaries of α and β, since domain γ is entered directly upon heating a system with composition φ_{2A} (Figures 2III and 8a). Following trace 1, however, we expect a small and rather broad first endotherm, due to the shape of α. There is a gradual release of the heat of demixing. Upon passing the three-phase line one of the two coexisting-phase concentrations jumps (see tie lines in Figure 2III), φ_{2A} changes drastically to φ_{2B}. A sudden change like that proceeds in a small temperature range so that most of the heat of demixing is liberated within a few degrees and, consequently, the signal will be sharp. Such behavior was found in the experiments performed with solutions of PVME 2 at $w_2 < 0.25$, an example of which is illustrated in Figure 3. The resolution of the two signals is better with the lower scanning rate. We have observed in previous experiments that a single endotherm is found at higher scanning rates where such details may easily be missed.[9] At concentrations in the immediate neighborhood of φ_{2A}, double peaks should occur, but the first one will usually be so small that it escapes detection (Figure 8a). Figures 3, 4, and 8 demonstrate that the system water/PVME consistently shows the behavior described above.

Double endotherms were observed in the high concentration range of both PVME samples but in the low concentration range only with PVME 2. It was not possible to observe two separate endotherms in the low concentration region with PVME 1, probably because of the small size of the endotherms.

2. Turbidimetry. Cloud points were measured for PVME 2 at a concentration between 0.2% and 60%, at a heating rate of 0.1°C/min. The results are shown in the phase diagram for PVME 2, illustrated in Figure 4.

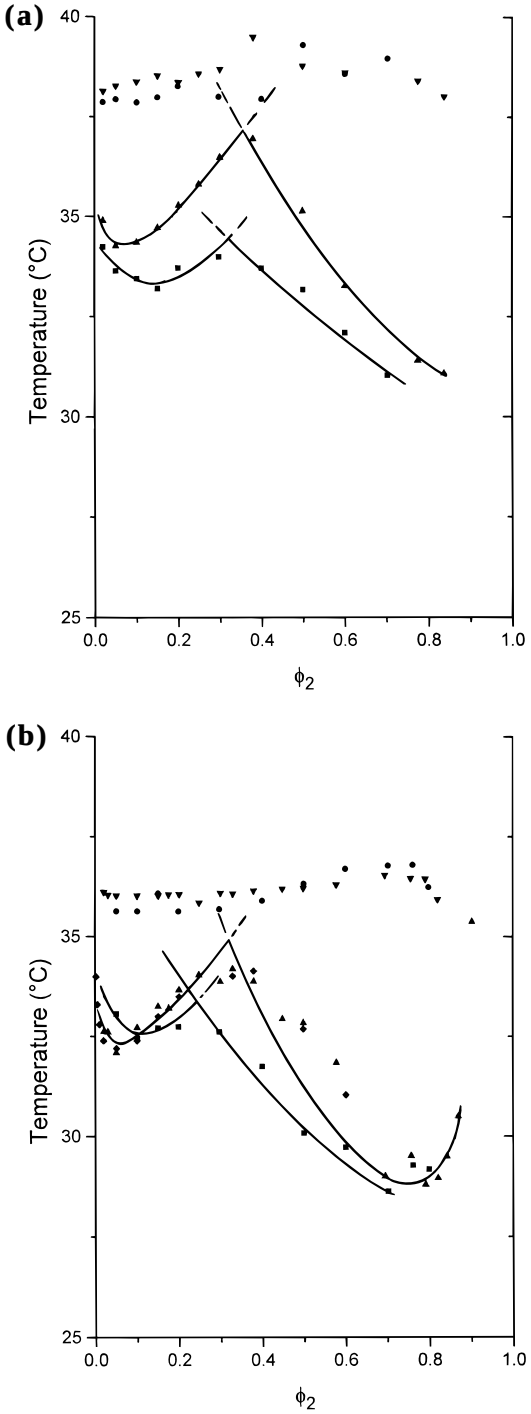

Figure 4. Phase diagrams derived from DSC measurements (curves hand-drawn): demixing temperature, T_d; peak temperature, T_p; scanning rates, (a) 3 °C/min, (b) 0.1 °C/min. PVME 1: ●, T_p; ■, T_d. PVME 2: ▼, T_p; ▲, T_d. Cloud points PVME 2: ◆. Polymer weight fraction, w_2.

The observed cloud points match very well with the onset temperatures T_d determined by calorimetry at similar heating rates.

3. Phase Analysis. Additional support for the presence of two minima in the demixing curve came from the investigation of the phase-volume ratio and the location of the coexistence curves in the α concentration region for PVME 2 (see Figure 2III). Solutions in this concentration region separate within a short time in two macroscopic, transparent layers on heating. The composition of these two phases and their volume ratio could be easily determined. The lower temperature limit for the observation of this phase separation was

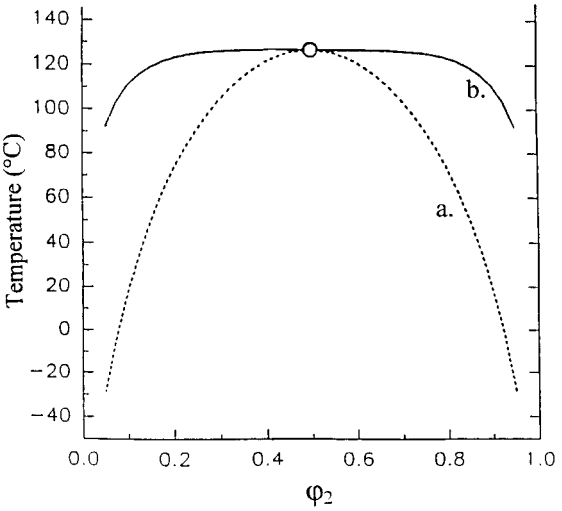

Figure 5. Miscibility gaps in symmetrical UCST systems ($m_1 = m_2 = 1$) calculated with eqs 1−3 and 7 for (a) $g_{0s} = 0$, $g_{0h} = 800$ K, $g_1 = 0$, $g_2 = 0$ and (b) $g_{0s} = -5$, $g_{0h} = 3067$ K, $g_1 = -4/3$, $g_2 = {}^4/_3$ Critical point, ○.

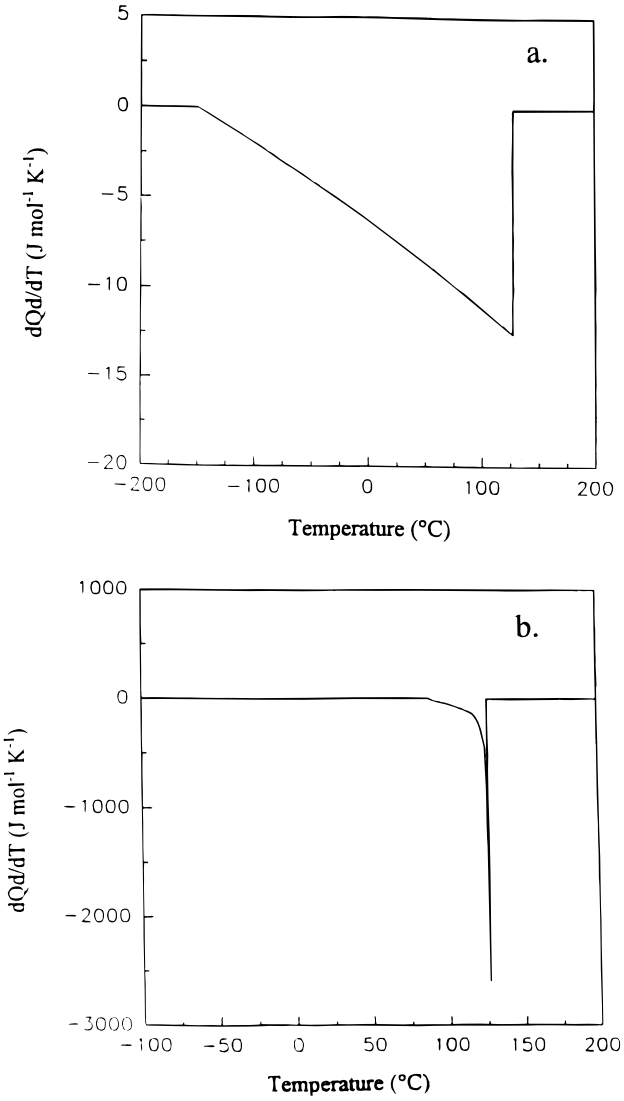

Figure 6. Simulations of DSC scans for cooling of systems a and b in Figure 5 at $\varphi_2 = 0.5$.[36]

33.5 °C for solutions with overall polymer concentrations of 4% and 6% and 34 °C for solutions with a higher polymer content. At 33 °C, only a haze is formed in these more concentrated solutions. The coexisting

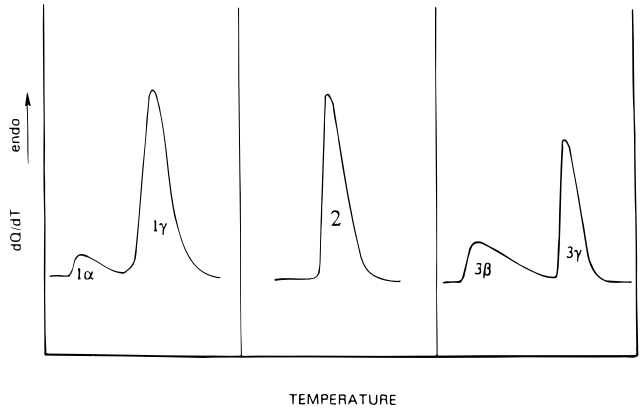

Figure 7. Appearance of DSC scans for heating routes 1−3 in Figure 2III.

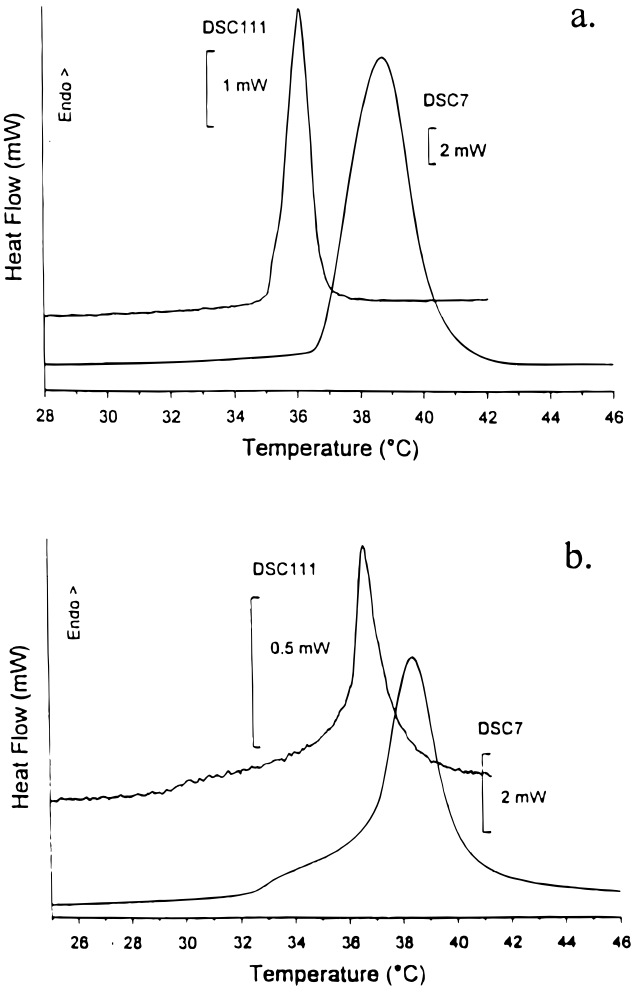

Figure 8. DSC curves for PVME2 at (a) 30.0 and (b) 77.5 wt % polymer.

concentrations are represented in Figure 9. The course of the coexistence curves for different overall polymer concentrations could be estimated and is indicated by hand-drawn lines for $T \leq 35$ °C. The above mentioned concentration jump is exemplified by the data points at 37 °C for which the copurse of the concentrated branches of the coexistence curves could only be indicated. The jump from $w_2 = 0.25$ to 0.6 within 2 °C is too large to be reasonably assigned to an unusual course of the coexistence curve.

The phase-volume ratio can be calculated from the curve of the coexisting concentrations. An excellent

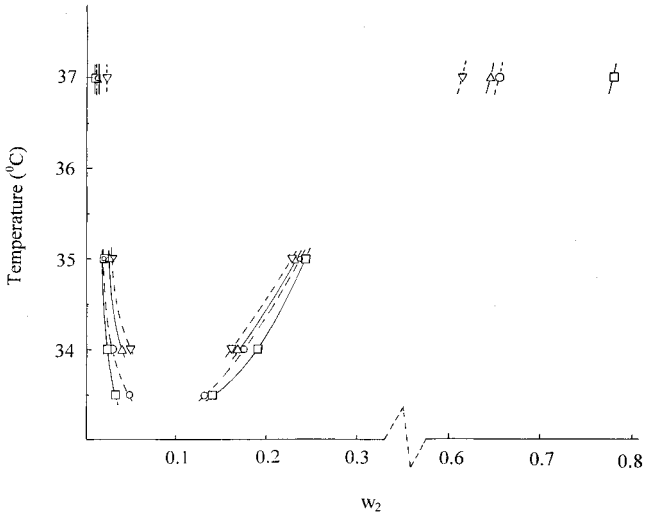

Figure 9. Coexistence curves for PVME 2 in water. Curves hand-drawn. Polymer weight fractions: 0.04, □; 0.06, ○; 0.08, △; 0.1, ▽.

Table 2. Phase Volume Ratios (Volume Dilute Phase/ Volume Concentrated Phase) for a 10% PVME 2 Sample, Recorded at Different Temperatures

temp (°C)	volume ratios from direct measurements	volume ratios from refractive index
34	1.2	1.27
35	1.8	1.82
36	3.2	

agreement is obtained with the phase-volume ratios obtained by direct observation (Table 2).

4. Enthalpy of Demixing. Integration of the shaded area in Figure 3 gives the enthalpy of demixing for the considered concentration. Plotted as a function of the polymer concentration these enthalpy data are reported in Figure 10 for PVME 2. A good agreement with literature data is obtained.[44]

Discussion

The present results establish that the system water/ PVME exhibits type III demixing behavior, indications for unusual phase relations already having been suggested by Tanaka.[46] Measurement by different methods, dynamic and static, demonstrate consistently that the miscibility gap is bimodal at large enough average molar mass of the polymer. This involves the existence of three two-phase areas, arranged around a narrow three-phase range, in accordance with classic rules.[31]

The pattern of the concentrations of the conjugate phases in Figure 9 agrees with the quasi-binary nature of the PVME solutions in hand. The measurement at 37 °C demonstrates the concentration jump, indicative for the passing of a three-phase range, as is also revealed by the concentration-insensitive major DSC peak temperatures (Figure 4). The peak temperatures occur about 1−2 °C higher than those of the intersections of gaps α and β. The onset temperatures of the sharp peak should have been plotted, but remain hidden by the first endotherm. A rough estimation indicates that an error of 1−2 °C may indeed be involved (Figures 3 and 8).

It is seen in Figure 4b that the size of gap α is smaller for PVME 1 than for PVME 2. Also, the minimum of gap β exhibits the insensitivity to molar mass indicated by theory. The right-hand boundaries of gap α intersect in a fashion that may reflect the different degree of

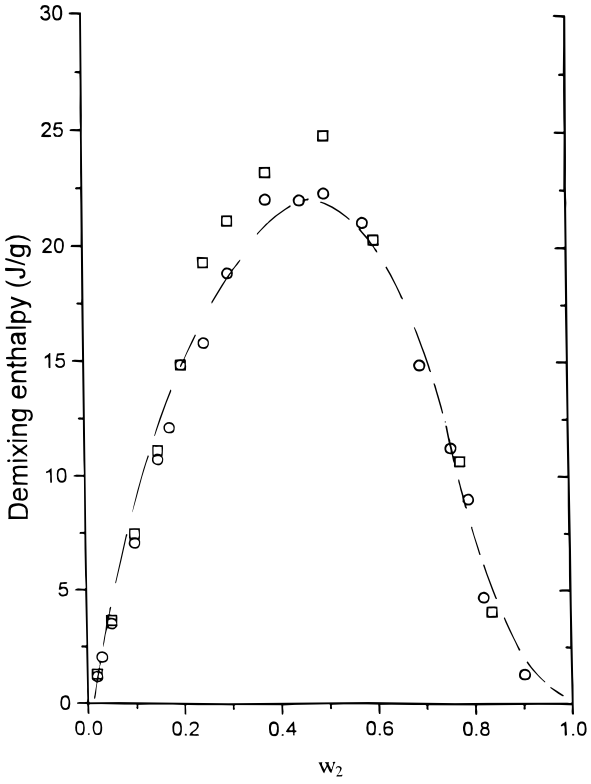

Figure 10. Enthalpy exchange per gram of solution for water/ PVME 2. Heating rates: 3 °C/min, □; 0.1 °C/min: ○. Weight fraction polymer: w_2.

polydispersity which is larger in PVME 2 than in PVME 1.[33] A quantitative study of the effect of the molar-mass distribution is currently being carried out.[8] A recent analysis of liquid/liquid phase behavior in the system acetone/polystyrene indicates the relevance of the present considerations for that system as well.[47] The parameter values presented in ref 47 point to type III behavior.

Acknowledgment. The authors are indebted to Prof. Burghard Schmitt and Dr. Schwarzenbach (BASF, Ludwigshafen) for kindly supplying the PVME samples and their molecular characterization. Miss Sabine Govaers (Catholic University Leuven) is thanked for preliminary measurements. The authors thank the Flemish Institute for the promotion of Scientific-Technological Research in Industry (IWT) for a fellowship for R.M. We also thank the National Fund for Scientific Research and the Fund for Collective and Fundamental Research, as well as the Ministry for Scientific Programmation through IUAP -II-16 for financial support. K. Š. thanks the U.S.−Czech Science and Technology Joint Fund, Project Number 95 024, for partial support.

References and Notes

(1) Flory, P. J. *Principles of Polymer Chemistry*, Cornell University Press: Ithaca, NY, 1953; Chapter XIII.
(2) Flory, P. J.; Daoust, H. *J. Polym. Sci.* **1957**, *25*, 429.
(3) Dušek, K. *Collect. Czech. Chem. Commun.* **1969**, *34*, 3309.
(4) Koningsveld, R.; Kleintjens, L. A. *Pure Appl. Chem., Macromol. Chem.* **1973**, *8*, 197.
(5) Nies, E.; Koningsveld, R.. Kleintjens, L. A. *Progr. Colloid Polym. Sci.* **1985**, *71*, 2.
(6) Moerkerke, R.; Koningsveld, R.; Berghmans, H.; Dušek, K.; Šolc, K. *Macromolecules* **1995**, *28*, 1103.
(7) Šolc, K.; Dušek, K.; Koningsveld, R.; Berghmans, H. *Collect. Czech. Chem. Commun.* **1995**, *60*, 1661.
(8) Ongoing work in the Laboratory for Polymer Research, Leuven University
(9) Govaers, S. Ph.D. work in progress.

(10) Gibbs, J. W. *The Scientific Papers*, Dover Reprint, 1961; Vol. I.: *Thermodynamics*.
(11) Stockmayer, W. H. *J. Chem. Phys.* **1949**, *17*, 588.
(12) Koningsveld, R. *Discuss. Farad. Soc.* **1970**, *No. 49*, 145.
(13) Šolc, K.; Kleintjens, L. A.; Koningsveld, R. *Macromolecules* **1984**, *17*, 573.
(14) Staverman, A. J.; Van Santen, J. H. *Rec. Trav. Chim.* **1941**, *60*, 76.
(15) Staverman, A. J. *Rec. Trav. Chim.* **1941**, *60*, 640.
(16) Huggins, M. L. *J. Chem. Phys.* **1941**, *9*, 440.
(17) Huggins, M. L. *Ann. N.Y. Acad. Sci.* **1942**, *43*, 1.
(18) Flory, P. J. *J. Chem. Phys.* **1941**, *9*, 660.
(19) Flory, P. J. *J. Chem. Phys.* **1942**, *10*, 51; **1944**, *12*, 425.
(20) Staverman, A. J. *Rec. Trav. Chim.* **1937**, *56*, 885.
(21) Koningsveld, R.; Kleintjens, L. A.; Leblans-Vinck, A. M. *J. Phys. Chem.* **1987**, *91*, 6423.
(22) Flory, P. J. *J. Am. Chem. Soc.* **1965**, *87*, 1833.
(23) Jain, R. K.; Simha, R. *Macromolecules* **1980**, *13*, 1501.
(24) Beckman, E. J.; Porter, R. S.; Koningsveld, R. *J. Phys. Chem.* **1987**, *91*, 6429.
(25) Coleman, M. M.; Graf, J. F.; Painter, P. C. *Specific Interactions and the Miscibility of Polymer Blends*; Technomic Publ. Co.: Lancaster, PA, 1991.
(26) Koningsveld, R. *Macromol. Symp.* **1994**, *78*, 1.
(27) Koningsveld, R.; Stockmayer, W. H.; Kennedy, J. W.; Kleintjens, L. A. *Macromolecules* **1974**, *7*, 73.
(28) Ten Brinke, G.; Szleifer, I. *Macromolecules* **1995**, *28*, 5434.
(29) Yamakawa, H. *Modern Theory of Polymer Solutions*; Harper & Row: New York, 1971.
(30) Šolc, K.; Koningsveld, R. *J. Phys. Chem.* **1992**, *96*, 4056.
(31) Schreinemakers, F. A. H. In *Die heterogenen Gleichgewichte vom Standpunkte der Phasenlehre*; Bakhuis Roozeboom, H. W. B., Ed.; Vieweg: Braunschweig, 1913; Vol. III, Part 2.
(32) Koningsveld, R.; Staverman, A. J. *Koll. Z. Z. Polym.* **1967**, *218*, 114.
(33) Koningsveld, R. *Adv. Colloid Interface Sci.* **2**, *2*, 151.
(34) Vandeweerdt, P. Ph.D. Thesis, Leuven, 1993.
(35) Buthenuth, M.; Jenckel, E. *Naturwissenschaften* **1956**, *43*, 276.
(36) Arnauts, J.; De Cooman, R.; Vandeweerdt, P.; Koningsveld, R.; Berghmans, H. *Thermochim. Acta* **1994**, *238*, 1.
(37) Arnauts, J.; Berghmans, H. *Polym. Commun.* **1987**, *28*, 66.
(38) Arnauts, J.; Berghmans, H. *Physical networks, polymers and gels;* Burchard, W., Ross Murphy, S. B., Eds.; **1990**, pp 33.
(39) Arnauts, J.; Berghmans, H.; Koningsveld, R. *Makromol. Chem.* **1993**, *194*, 77.
(40) Vandeweerdt, P.; Berghmans, H.; Tervoort, Y. *Macromolecules* **1991**, *24*, 3457.
(41) Berghmans, H.; Deberdt, F. *Phil. Trans. R. Soc. London A* **1994**, *348*, 117.
(42) Callister, S.; Keller R.; Hikmet, R. M. *Makromol. Chem., Macromol. Symp.* **1990**, *39*, 19.
(43) Vandeweerdt, P.; Decooman, R.; Berghmans, H.; Meijer, H. *Polymer* **1994**, *35*, 5141.
(44) Maeda, H. *J. Polym. Sci., Polym. Phys. Ed.* **1994**, *32*, 91.
(45) Soenen, H.; Berghmans, H. *J. Polym. Sci., Polym. Phys. Ed.* **1995**, *33*, in press.
(46) Tanaka, H. *4th SPSJ Int. Polym. Conf.* **1992**, 160.
(47) Vanhee, S.; Koningsveld, R.; Berghmans, H.; Šolc, K. *J. Polym. Sci., Polym. Phys. Ed.* **1994**, *32*, 2307.

MA960114O